



Unsupervised hierarchical image segmentation with level set and additive operator splitting

M. Jeon^a, M. Alexander^a, W. Pedrycz^b, N. Pizzi^{a,*}

^a *Institute for Biodiagnostics, National Research Council, 435 Ellice Avenue, Winnipeg, MB, Canada R3B 1Y6*

^b *Department of Electrical and Computer Engineering, University of Alberta, Edmonton, AB, Canada*

Received 28 September 2004

Available online 18 December 2004

Abstract

This paper presents an unsupervised hierarchical segmentation method for multi-phase images based on a single level set (2-phase) method and the semi-implicit additive operator splitting (AOS) scheme which is stable, fast, and easy to implement. The method successively segments image subregions found at each step of the hierarchy using a decision criterion based on the variance of intensity across the current subregion. The segmentation continues until a specified number of levels has been reached. The segmentation information for sub-images at each stage is stored in a tree data structure, and is used for reconstructing the segmented images. The method avoids the complicated governing equations of the multi-phase segmentation approach, and appears to converge in fewer iterations. The method can easily be parallelized because the AOS scheme decomposes the equations into a sequence of one dimensional systems.

© 2004 Elsevier B.V. All rights reserved.

Keywords: Image processing; Hierarchical segmentation; Variational PDE; Level set methods; Additive operator splitting

1. Introduction

Segmentation is the important technique for detecting objects and analyzing images in the com-

puter vision and image processing fields. Segmentation methods fall into several categories; we will consider the following: (1) histogram analysis, (2) region growing, (3) edge detection, and (4) partial differential equations (PDE)-based methods. For a more comprehensive discussion, see the references (Cheng et al., 2001; Jahne, 2002; Russ, 2003).

The histogram analysis method (Russ, 2003) segments an image based on the distribution of its intensity and a pre-defined set of thresholds. This method does not make use of spatial structural

* Corresponding author. Tel.: +1 204 983 8842; fax: +1 204 984 5472.

E-mail addresses: moon-gu.jeon@nrc-cnrc.gc.ca (M. Jeon), murray.alexander@nrc-cnrc.gc.ca (M. Alexander), pedrycz@ee.ualberta.ca (W. Pedrycz), nick.pizzi@nrc-cnrc.gc.ca, pizzi@cs.unmanitoba.ca (N. Pizzi).

information, so it is effective for simple images that display only small amounts of structure.

Edge-based segmentation methods (Jahne, 2002) find the edges of objects in the image, and use this edge information to reconstruct complete boundaries for the principal objects in the image. It is based on the fact that the position of an edge is given by an extreme of the first-order derivative or a zero crossing in the second-order derivative. Its main drawback is that the true edges are fragmented by noise in the image. Sobel and Canny algorithms belong to this group.

Region growing (Gonzalez and Woods, 2002) is one of the most popular segmentation methods. It segments an image by splitting the image into smaller regions and merging them into larger ones with k -means, k -nearest neighborhood or some other clustering method. Merging or grouping criteria may be based on criteria such as homogeneity, proximity, color, gray level or texture. To some extent it solves the noise problem related to the edge detection method, and out-performs histogram methods in almost all situations. However, this method still has several disadvantages. Among them, its high computational complexity is the most serious. Many approaches use some combination of these and other methods. For example, the watershed segmentation algorithm uses a combination of region growing and edge-based approaches, producing more stable segmentation results (Gonzalez and Woods, 2002).

The PDE and variational based methods (Morel and Solimini, 1995) are the most recently developed of the methods for image segmentation. The main advantage is that the theory behind the concept and the solution techniques are well established in other fields such as physics and mechanics (Aubert et al., 2002). The snake (Kass et al., 1987), the gradient vector flow (Xu and Prince, 1998) and the level set method (Osher and Sethian, 2003), are typical of the methods belonging to the class of PDE-based methods. The level set method is one of the most powerful tools for capturing boundaries or tracking interfaces in image processing and material science. To track interfaces, the function describing the interfaces is defined implicitly by a partial differential equation, and solved numerically.

The method of active contours without edges (Chan and Vese, 2001) is based on a variational principle. The objective functional is the one formulated by Mumford and Shah (1989), and is written in terms of the level set function (which determines the contour). It incorporates the length of interfaces, and variation of the individual pixel intensities inside and outside the interface. The level set function is found as a solution of the corresponding Euler–Lagrange equations, and is obtained numerically using a gradient descent method (Strikwerda, 1989). These authors also developed multi-level set models (Vese and Chan, 2002) for multi-phase segmentation based on the active contour (piecewise constant case) and the Mumford–Shah model (piecewise smooth case). Their models can segment 2^n phases of the image, where n is the number of level set functions. Thus, the multi-phase C–V model evolves more regions than necessary whenever the number of regions is not a power of two. In this case, the redundant regions are empty. For example, a 5-phase image requires 3 level set functions, which produces 8 sub-images of which 3 are empty. Therefore, although this method still produces correct results, it does so at the expense of unnecessary and time-consuming computation.

Tsai et al. (2001) have employed a hierarchical approach to relieve the complexity of the multi-phase level set methods based on the Mumford–Shah model. Our method is similar to theirs but differs with respect to user intervention and solution technique. While their method requires user intervention at each stage of segmentation, ours automatically selects a subregion using intensity variations as the decision criterion, and employs a multi-scale analysis with wavelets for fast processing.

The paper is organized as follows. The next section reviews the basic level set 2-phase segmentation model developed by Chan and Vese (2001) and the additive splitting operator developed by Weichert et al. (1998). Section 3 describes our unsupervised hierarchical segmentation algorithm in detail, and then provides some test results in Section 4. Finally, conclusions and future research directions are presented.

2. Level set formulation and additive operator splitting

Our method is based on the model of active contours without edges for two-phase problems by Chan and Vese (2001) (C–V model), where the energy functional involves the length of interfaces, area (volume for 3-D), and two fitting terms, written as

$$\begin{aligned} E(C_1, C_2, \phi) = & \mu \int_{\Omega} \delta(\phi) |\nabla \phi| dx \\ & + \nu \int_{\Omega} H(\phi) dx \\ & + \lambda_1 \int_{\Omega} |u_0(x) - C_1|^2 H(\phi) dx \\ & + \lambda_2 \int_{\Omega} |u_0(x) - C_2|^2 (1 - H(\phi)) dx, \end{aligned}$$

where Ω is the image domain, ϕ represents an implicit function of the interface, C_1 and C_2 represent the average intensities of inside and outside interfaces, respectively, H the Heaviside function and δ is the Dirac function: $\delta(\phi) = \frac{dH(\phi)}{d\phi}$.

The positive parameters μ , ν , λ_1 and λ_2 are fixed, and define the relative weightings given to the various terms in the above functional. Minimizing with respect to its parameters (C_1, C_2, ϕ) gives the following three Euler–Lagrange equations over the domain Ω :

$$|\nabla \phi| \left[\mu \nabla \cdot \left(\frac{\nabla \phi}{|\nabla \phi|} \right) - \nu - \lambda_1 (u_0 - C_1)^2 + \lambda_2 (u_0 - C_2)^2 \right] = 0, \quad (1)$$

$$C_1(\phi) = \frac{\int u_0(x) H(\phi(x)) dx}{\int H(\phi(x)) dx}, \quad (2)$$

$$C_2(\phi) = \frac{\int u_0(x) (1 - H(\phi(x))) dx}{\int (1 - H(\phi(x))) dx}. \quad (3)$$

Eq. (1) can be solved either directly by an optimization technique (Chan et al., 1995), or by transforming it to an evolution equation (Rudin et al., 1992). The former method is rarely used, and the latter, which we use in this paper, formulates the evolution equation with initial and boundary

conditions as the gradient descent method, as follows:

$$\begin{aligned} \frac{\partial \phi}{\partial t} = & |\nabla \phi| \left[\mu \nabla \cdot \left(\frac{\nabla \phi}{|\nabla \phi|} \right) - \lambda_1 (u_0 - C_1)^2 \right. \\ & \left. + \lambda_2 (u_0 - C_2)^2 \right], \end{aligned} \quad (4)$$

$$\phi(x, 0) = \phi_0(x), \quad (5)$$

$$\frac{\partial \phi(x)}{\partial n} = 0, \quad x \in \partial \Omega: \text{ boundary of image.} \quad (6)$$

Following (Chan and Vese, 2001), we replace $|\nabla \phi|$ by the approximation to the delta function $\delta_h(\phi) = \frac{\partial}{\partial \phi} \frac{1}{2} (1 + \frac{2}{\pi} \tan^{-1}(\frac{\phi}{h}))$ which leads to more effective implementation:

$$\begin{aligned} \frac{\partial \phi}{\partial t} = & \delta_h(\phi) \left[\mu \nabla \cdot \left(\frac{\nabla \phi}{|\nabla \phi|} \right) - \lambda_1 (u_0 - C_1)^2 \right. \\ & \left. + \lambda_2 (u_0 - C_2)^2 \right]. \end{aligned} \quad (7)$$

As the time $t \rightarrow \infty$, $\frac{\partial \phi}{\partial t} \rightarrow 0$, which gives the solution to the Euler–Lagrange equation (1). Usual choices of λ_1 and λ_2 are 1, ν is 0, and the parameter μ controls the size of captured objects. With small μ small objects are captured, and with larger μ only larger objects are captured. The above analysis can easily be extended to multi-channel images (Chan et al., 2000).

The system equations of multi-phase level sets can be derived by adding more level sets as variational parameters in the energy functional E (Vese and Chan, 2002). However, as the number of level sets increases, the system of governing equations becomes more complicated, and their numerical solution more difficult to obtain on account of slow convergence of the iterations.

An explicit scheme is the most popular for solving Eq. (7), but due to the Courant–Friedrichs–Lewy (CFL) condition which asserts that the numerical waves should propagate at least as fast as the physical waves (Osher and Fedkiw, 2003), it requires very small time steps and therefore a large number of iterations. Instead, we apply the semi-implicit additive operator splitting (AOS) scheme by Weichert et al. (1998), which remains

numerically stable for large time steps and converges in fewer iterations. We briefly review its basic idea; more details can be found in (Weichert et al., 1998). The AOS scheme splits the m -dimensional spatial operator into a sum of m one-dimensional space discretizations. The update of each grid point involves only two neighbors in each dimension, thus reducing the system to a set of tridiagonal equations. The numerical solution of each tridiagonal system requires $O(3N_i)$ floating point operations where N_i is the number of pixels along the i th coordinate axis, and there are $\frac{N}{N_i}$ such systems for each $i = 1, \dots, m$, giving a total of $O(3Nm)$ float operations per iteration, where $N = \prod_{i=1}^m N_i$ is the total number of pixels in the image. The Thomas algorithm (Weichert et al., 1998) is used to solve the underlying tridiagonal system, resulting in a very fast and parallelizable algorithm. This is possible since the data for each tridiagonal system is completely independent. Let k and i represent time and spatial indices, respectively. Let $f = \frac{1}{|\nabla\phi|}$, then f_i^k is the value of f at spatial (grid) point i and time k . At grid point i , the 1-dimensional semi-implicit discretization of equation (7) is

$$\frac{\phi_i^{k+1} - \phi_i^k}{dt} = \delta_h(\phi_i^k) \left(\frac{f_i^k + f_{i+1}^k}{2h} \frac{\phi_{i+1}^{k+1} - \phi_i^{k+1}}{h^2} - \frac{f_i^k + f_{i-1}^k}{2h} \frac{\phi_i^{k+1} - \phi_{i-1}^{k+1}}{h^2} + F_i \right),$$

where $F_i = [\lambda_1(u_{0,i} - C_1)^2 - \lambda_2(u_{0,i} - C_2)^2]$, which can be rearranged as

$$\phi_i^{k+1} = \phi_i^k + \frac{dt}{h^2} (b\phi_{i+1}^{k+1} - a\phi_i^{k+1} + c\phi_{i-1}^{k+1} + F_i),$$

where $dt =$ time step, $h =$ space step, and

$$a = \delta_h(\phi_i^k) \frac{f_{i-1}^k + 2f_i^k + f_{i+1}^k}{2},$$

$$b = \delta_h(\phi_i^k) \frac{f_i^k + f_{i+1}^k}{2},$$

$$c = \delta_h(\phi_i^k) \frac{f_i^k + f_{i-1}^k}{2}.$$

To avoid a singularity of $\frac{1}{|\nabla\phi|}$, it is slightly perturbed (Osher and Fedkiw, 2003)

$$\frac{1}{|\nabla\phi|} \approx \frac{1}{\sqrt{(\nabla\phi_x)^2 + \epsilon}},$$

where ϵ is a small number (10^{-7} which is used in our implementation).

3. Unsupervised hierarchical segmentation

This section describes an unsupervised hierarchical segmentation algorithm using the active contour model. As mentioned above, the C–V segmentation model works well for two-phase problems. Unlike (Chan and Vese, 2001), we now extend it to multi-phase problems. We use only one level set equation. Suppose we want to segment the image into three phases. After the first step, the one-level set method captures one phase as an object, and its complement as background. The intensity variation across the captured object and its complementary background is compared, and the one having the larger variation becomes the target for the next step of the hierarchy. The region of smaller intensity variation is then replaced with a uniform intensity (already computed as the parameter C_1 or C_2) equal to the average intensity of the region having the larger intensity variation. This effectively excludes the region of smaller intensity variation from being re-segmented at the next step of the hierarchy. The above procedure is repeated on the resulting image. Note that this image has the same dimensions as the initial input image, so that at each step the segmentation is carried out on the same size of image. After this second step, the image will be partitioned into 3 phases. The entire hierarchical procedure can be represented as a binary tree (Fig. 1), with regions represented as nodes and children of each node being created by a single step of the one-level set segmentation procedure. The set of leaves of this tree constitutes the final segmentation of the original image into a number of phases equal to the number of leaves. Even though the method's use of the entire image at each segmentation step results in redundant computation, it has the advantage of using a simple boundary (namely, the boundary $\partial\Omega$ of the full-size image) at each step. Now we define a decision criterion for branching at a node.

Definition 1 (Intensity Variation). Let I denote a given image, and S_1, S_2, \dots, S_n denote a partition

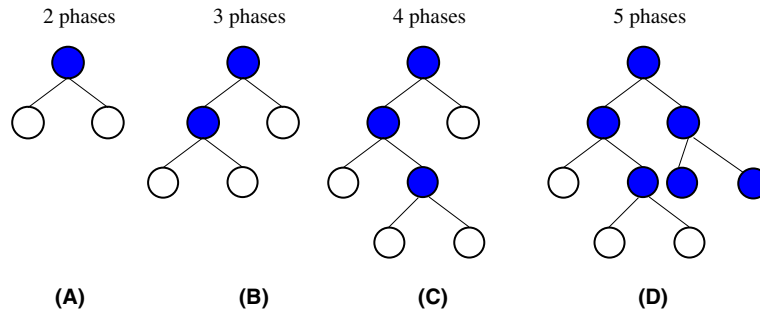


Fig. 1. Binary tree structure of hierarchical segmentation.

of I , formed by segmentation using the single level set method. Then the intensity variation across S_i is defined as

$$\text{Var}(S_i) = \frac{1}{M_i} \sum_{k=1}^{M_i} (I(x_k, y_k) - C_i)^2,$$

where C_i (defined in Section 2) represents the average intensity of sub-image S_i , and M_i represents the number of pixels in the sub-image S_i .

We note that the defined intensity variation measures the deviation from homogeneity of the subregion of the image. Thus, the sub-image with larger variation can be further segmented into more phases, and will be the next target for segmentation. Based on the above reasoning we can segment multi-phase images hierarchically with just a single level set function as described in Algorithm 1 where the only data a user should provide are the number of phases of the given image and the initial contour.

Algorithm 1 (unsupervised hierarchical segmentation).

```

nos: given number of segmentation phases
u0: given image
p0: initial contour
 ← u0
L: left child (sub)image
R: right child (sub)image
for i = 1:nos do
    p ← p0
    [p,L,R] ← level_set_solver(p,)
    
```

Find a leaf (*subI*) with smallest intensity variation (Definition 1).

$Img \leftarrow subI$ and replace its complement by the C value belonging to $subI$

end for

To illustrate this algorithm, we show in Fig. 1 an example of a hierarchy of a 5-phase image segmentation. Each leaf contains information, i.e. the intensity variation and pixel indices on one sub-image. The root (given image) branches into two nodes of sub-images (A), and the left sub-image is chosen for branching by our selection criteria of the intensity variation. After finishing segmentation of the left node, we now have three leaves of sub-images (B). If the number of phases or clusters required is 3, then we stop here since three leaf nodes are decided. Otherwise, the algorithm compares the variations of all current leaves to decide which one should be segmented, and repeats branching until the required number of leaves are produced ((C) and (D)).

Some test results are given in the next section.

4. Experiment

Our algorithm is applied to the segmentation of two artificial images and a real magnetic resonance (MR) brain image. In all cases, the initial conditions for the 0-level set are chosen as a large number of small circles covering the image domain, which gives fast convergence to the solution contour.

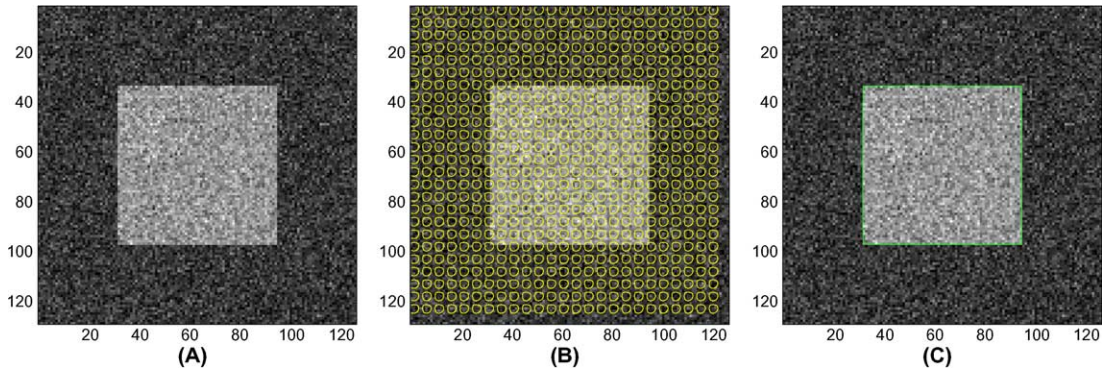


Fig. 2. Two-phase noisy artificial image segmentation: (A) noisy 2-phase image, (B) initial 0-contour, (C) 2 phases segmentation.

First, a simple 2-phase noisy image is tested with our method for robustness to noise. The robustness property is inherited from Eq. (7) (Chan and Vese, 2001). In Fig. 2, the first image is the original one, and the second displays the multi-circle initial condition of the 0-level set. The third image shows the successful segmentation of the target object. It was found that as the signal-to-noise ratio decreases, the algorithm takes a greater number of iterations to converge. Alternatively, we could choose a larger time step to reduce the number of iterations, which cannot be achieved by the explicit scheme (see Section 2).

The second test was carried out with three phases on an artificial noisy image. The first figure in the top row of Fig. 3 contains an initial contour (red circle)¹ on the given image. The second figure shows that the single level set method segments first phase objects enclosed by the green contour, but cannot capture objects whose intensity is close to that of background. In other words, at the first level of the hierarchy they are treated as the background. Our algorithm computes the intensity variations of the background and the captured objects, and decides that the background containing the objects should be segmented at the next stage. The third figure shows the successful segmentation of the remaining objects (enclosed by the red contour) from the background at the next stage of segmenta-

tion. To see the effectiveness of our algorithm, we compare it with the three common algorithms, Sobel and Canny in the Image Processing Toolbox of Matlab (Mathworks, 2003), and gradient vector flow (GVF) (Xu and Prince, 1998); the results are shown in the bottom row of Fig. 3. Sobel cannot recognize objects whose intensity is close to the background, and Canny captures both objects, but is heavily corrupted by the noise in the image: this makes the correct analysis of the image very difficult. GVF can successfully segment an individual object, but is not able to simultaneously segment disjoint objects (as shown by the red contour enclosing the bright segments in the lower right image in Fig. 3). Also as with Sobel, GVF is unable to capture objects closer in intensity to the background.

Our final example is the multi-phase segmentation of an MR brain image in Fig. 4. The brain is composed of cerebrospinal fluid (CSF), gray matter (GM), white matter (WM), skull and scalp, which appears as the bright outer ring. In practice, the important objects are CSF, GM and WM, but for the demonstration of multi-phase segmentation we try to segment all 5 phases. The first figure of the top row of Fig. 4 is the given MR brain image, and the second figure showing the initial contour of multiple circles. At the first stage of segmentation, most phases are captured as one object (green contour in the third figure of the first row), but some parts whose intensities are close to the background are not. Since the intensity variation of the captured object is greater than the background, the subregion inside the interface is processed at the

¹ For interpretation of colour please refer the web version of this article.

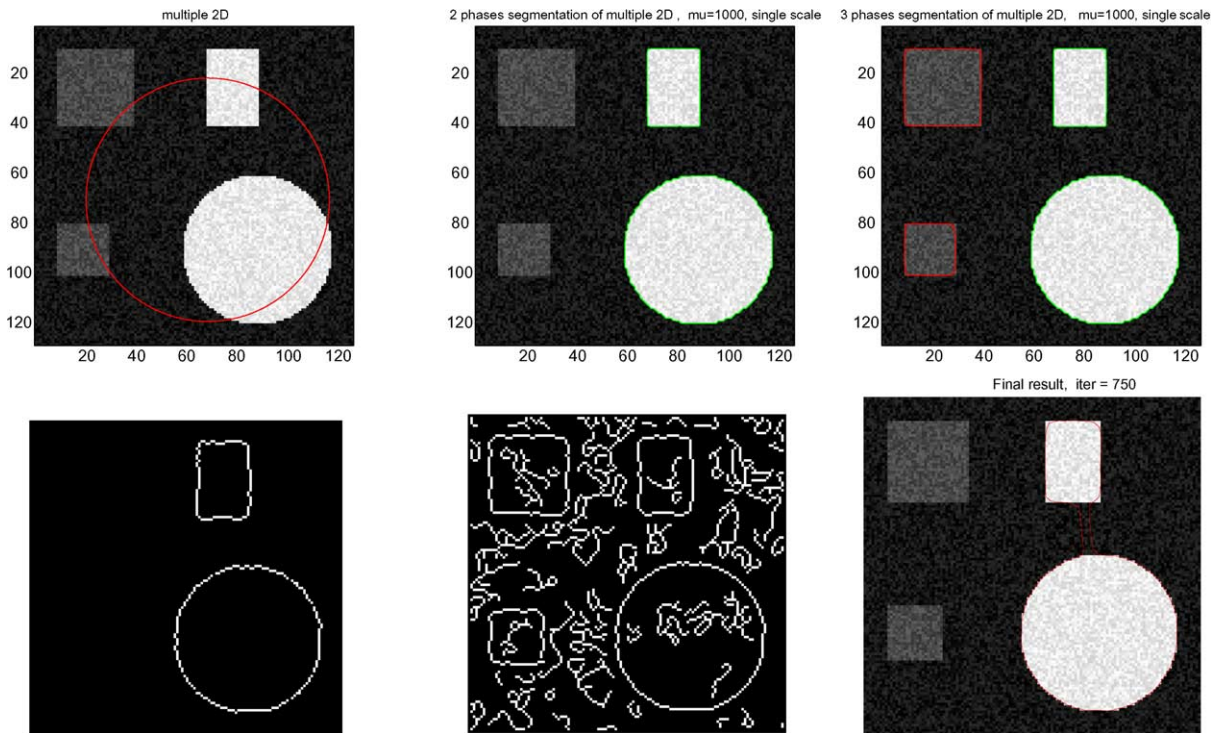


Fig. 3. Top row: from left, initial contour, 2 phases segmentation, 3 phases segmentation, bottom row: Sobel, Canny, GVF segmentation.

next stage ((B) of Fig. 1 and the lower left of Fig. 4). The procedure is repeated until all 5 phases are segmented. Segmentation of each phase is represented with the different coloured contour in Fig. 4. Notice that at the final stage it segments the sub-image which was chosen as the background at the first stage. See the tree structure in Fig. 1, which corresponds to this example.

5. Discussion and conclusion

Our method extends a single level-set (2-phase) method to a multi-phase method by using a single level-set hierarchically. At each step of this hierarchy, the background or unselected sub-image is replaced with the average intensity of the selected sub-image for the input of the next stage of segmentation. Test results show this strategy works very well, is robust to noise, and captures very small-scale details of multi-phase images. In the compari-

son with segmentation of three phases in a noisy image, we found that while Sobel does not capture some phases, Canny captures even spurious objects, and GVF has a problem with segmenting a group of objects. Our method overcame all the drawbacks of three methods. For hierarchical segmentation the method employs a simple criterion of comparing intensity variations within the current segmentation and its complement. The component with the smaller intensity variation is replaced by the mean intensity of its complement, and the algorithm proceeds to segment the resulting image as before. In this way, complex boundary conditions are avoided at the expense of a larger computational domain. That is, the size of input for each stage is the same as that of the first stage, even though the actual domain is reduced in size.

The principal contribution of our research is that, with a simple decision criterion and a hierarchical approach, the single level set segmentation method successfully extends to the multi-phase

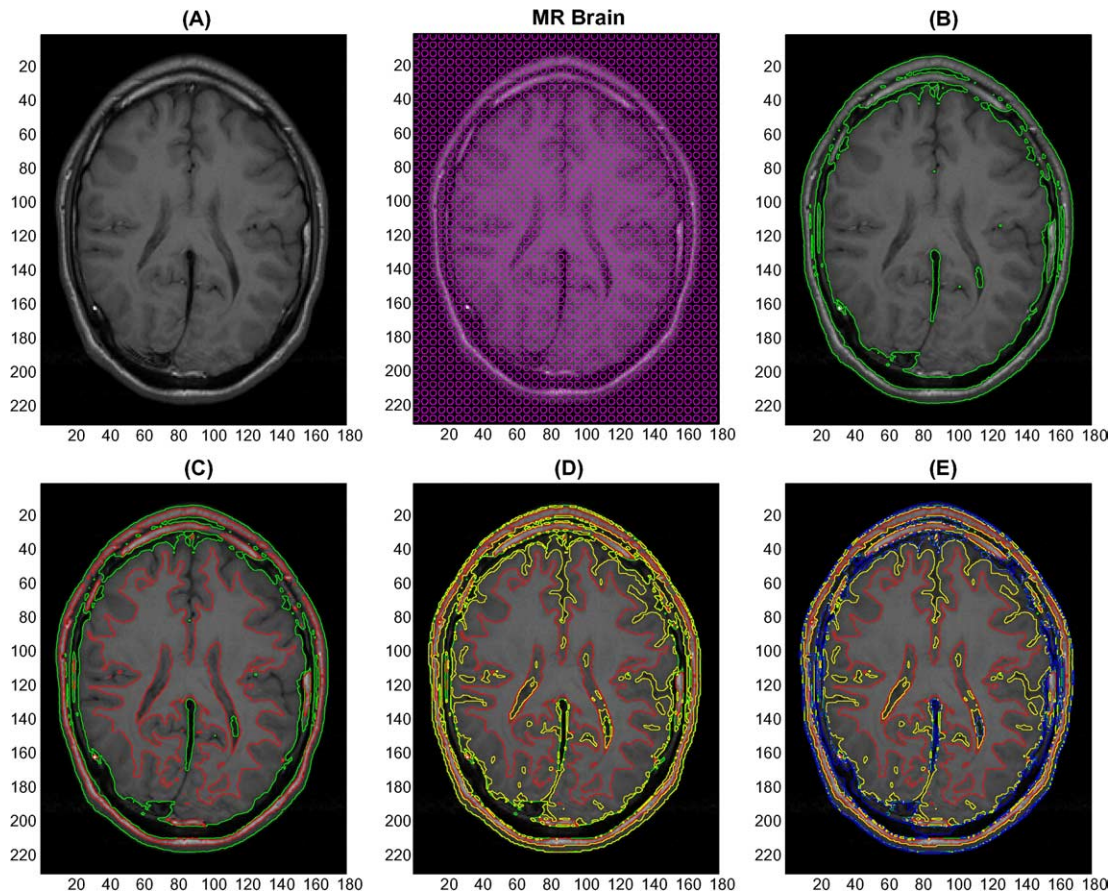


Fig. 4. Top row: given multi-phase MR brain Image, multiple initial contours, 2 phases segmentation (green), bottom row: 3 phases segmentation (red), 4 phases segmentation (yellow), 5 phases segmentation (blue) (for interpretation of colour please refer the web version of this article).

segmentation method. For fast and convenient processing, our algorithm will be parallelized and incorporated into the Scopira system (Demko et al., 2002) which was developed by the Institute for Biodiagnostics, NRC Canada, and which provides many optimized data structures, mathematical libraries, visualization tools, and GUIs. More improvement on computational time can be achieved by multi-scale analysis with wavelets for each stage of segmentation.

Acknowledgement

We thank the referees for their suggestion for improving the clarity and content of the paper.

This work was financially supported by NSERC (Natural Science and Engineering Research Council, Canada).

References

- Aubert, G., Kornprobst, P., 2002. *Mathematical Problems in Image Processing*. Springer, New York.
- Chan, T.F., Golub, J.H., Mulet, P., 1995. A Nonlinear Primal-Dual Method for Total Variation-Based Image Restoration. CLA Tech. Report, Sept. 1995.
- Chan, T.F., Sandberg, B.Y., Vese, L.A., 2000. Active contours without edges for vector-valued images. *J. Visual Commun. Image Representat.* 11 (2), 130–141.
- Chan, T.F., Vese, L.A., 2001. Active contours without edges. *IEEE Trans. Image Process.* 10 (2), 266–277.

- Cheng, H.D., Jiang, X.H., Sun, Y., Wang, J., 2001. Color image segmentation: Advances and prospects. *Pattern Recognition* 34, 2259–2281.
- Demko, A., Pizzi, N., Somorjai, R., 2002. Scopira—a system for the analysis of biomedical data. *Proceedings of IEEE Canadian Conference on Electrical and Computer Engineering*, Winnipeg, Canada, May 12–15. pp. 1093–1098.
- Gonzalez, R.C., Woods, R.E., 2002. *Digital Image Processing*. Prentice Hall.
- Jahne, B., 2002. *Digital Image Processing*. Springer.
- Kass, M., Witkin, A., Terzopoulos, D., 1987. Snakes: Active contour models. *1st International Computer Vision Conference*.
- Mathworks. *Image Processing Toolbox User's Guide*, 2003.
- Morel, J.M., Solimini, S., 1995. Variational methods in image segmentation. In: *Progress in Nonlinear Differential Equations and their Applications*. Birkhauser, Basel.
- Mumford, D., Shah, J., 1989. Optimal approximation by piecewise smooth functions and associated variational problem. *Commun. Pure Appl. Math.* 42, 577–685.
- Osher, S., Fedkiw, R., 2003. *Level Set Methods and Dynamic Implicit Surfaces*. Springer, New York.
- Osher, S., Sethian, J.A., 2003. Fronts propagating with curvature-dependent speed: Algorithms based on Hamilton–Jacobi formulations. *Journal of Computational Physics* 79, 12–49.
- Rudin, L.I., Osher, S., Fetami, E., 1992. Nonlinear total variation based noise removal algorithms. *Physica D* 60, 259–268.
- Russ, J.C., 2003. *The Image Processing Handbook*. CRC Press.
- Strikwerda, J.C., 1989. *Finite Difference Schemes and Partial Differential Equations*. CRC Press.
- Tsai, A., Yezzi, A., Willsky, A.S., 2001. Curve evolution implementation of the Mumford–Shah functional for image segmentation, denoising, interpolation, and magnification. *IEEE Trans. Image Process.* 10 (8), 1169–1186.
- Vese, L.A., Chan, T.F., 2002. A multiphase level set framework for image segmentation using the Mumford and Shah model. *Int. J. Comput. Vision* 50 (3), 271–293.
- Weichert, J., Romeny, B., Viergever, M.A., 1998. Efficient reliable schemes for nonlinear diffusion filtering. *IEEE Trans. Image Process.* 7 (3), 398–410.
- Xu, C., Prince, J.L., 1998. Snakes, shapes, and gradient vector flow. *IEEE Trans. Image Process.* 7 (3).